**SUPPORTING INFORMATION**

# Nanopore-based identification of individual nucleotides for direct RNA sequencing

*Mariam Ayub*[1], *Steven W. Hardwick*[2], *Ben F. Luisi*[2] *and Hagan Bayley*[1]*

[1]Department of Chemistry, University of Oxford, Oxford, OX1 3TA, United Kingdom.

[2]Department of Biochemistry, University of Cambridge, Cambridge, CB2 1GA, United Kingdom.

*Correspondence and requests for materials should be addressed to H.B. (email: hagan.bayley@chem.ox.ac.uk)

**Supporting Information Methods**

**Protein preparation.** Heptameric αHL proteins were produced as described[1] by E. Mikhailova in our laboratory. Aliquots of the purified protein were stored at -80°C.

**Mutagenesis.** Mutant αHL genes were prepared using a kit for site-directed mutagenesis (QuikChange II XL, Catalog no. 200522-5, Stratagene), and verified by sequencing[1]. M113R, M113N and M113F were made by using the RL2 gene as the template. The RL2 gene encodes four amino acid replacements in the barrel domain (Val-124 to Leu, Gly-130 to Ser, Asn-139 to Gln, Ile-142 to Leu) and one in the cap region of αHL (Lys-8 to Ala)[1, 2].

**αHL-$(N139Q)_6(N139Q/L135C)_1$.$am_6$-$amPDP_1$-βCD.** The αHL pore with a covalently attached cyclodextrin, αHL-$(N139Q)_6(N139Q/L135C)_1$.$am_6$-$amPDP_1$-βCD, was obtained from Oxford Nanopore Technologies[3]. This pore contains a functionalized cyclodextrin, heptakis(6-deoxy-6-amino)-6-N-mono(2-pyridyl)dithiopropanoyl-β-cyclodextrin ($am_6$am-$PDP_1$βCD), coupled to the Cys residue within the αHL $(N139Q)_6(N139Q/L135C)_1$ pore (Figure S7).

**PNPase preparation.** N-terminally His tagged *Caulobacter crescentus* polynucleotide phosphorylase (PNPase) was expressed and purified as described previously[4], Figure S8.

**$gu_7$βCD.** Heptakis(6-deoxy-6-guanidino)-βCD ($gu_7$βCD, >98%) was obtained from Oxford Nanopore Technologies. $gu_7$βCD was prepared by modification of the amino groups of heptakis(6-deoxy-6-amino)-β-cyclodextrin.7HCl ($am_7$βCD, Cyclolab) with 1H-pyrozolecarboxamidine, in the presence of di-isopropyl ethylamine[5] (Figure S2, Figure 2).

**Planar bilayer recording.** Electrical recordings were carried out with a planar lipid bilayer apparatus by using bilayers of 1,2-diphytanoyl-sn-glycero-3-phosphocholine (DPhPC, Avanti Polar Lipids) formed across an aperture (~100 μm in diameter) in a 25-μm thick polytetrafluoroethylene (Teflon) film (Goodfellow, Cambridge, Cat. #FP301200/10), which separated the apparatus into cis and trans compartments[6]. Bilayers were formed by first pre-treating the aperture with hexadecane in n-pentane (10 mg $mL^{-1}$). Unless stated otherwise, the electrolyte solution was the same in both compartments (symmetrical conditions (500 μL): 1 M KCl, 25 mM Tris.HCl at pH 7.5). Then, DPhPC in n-pentane (10 mg $mL^{-1}$) was added on both sides. The pentane was allowed to evaporate and a bilayer was formed by lowering and raising the electrolyte level past the aperture. When different buffer compositions were used (asymmetrical conditions), this is indicated in the text. All current recordings were performed with a patch clamp amplifier (Axopatch 200B, Molecular Devices) with the cis compartment connected to ground.

**rNDP identification with a non-covalently bound cyclodextrin adapter.** Reagents: 2-uridine 5-diphosphate disodium salt (rUDP, 99%, Fluka); cytosine 5-diphosphate (rCDP, >98%, Fluka); adenosine 5-diphosphate (rADP, 99%, Acros); guanosine 5-diphosphate disodium salt (rGDP, 97%, Acros); heptakis(6-deoxy-6-amino)-β-cyclodextrin.7HCl ($am_7$βCD, >99%, Cyclolab).

M113X-RL2 αHL pores and rNDPs (10 μM) were added to the cis compartment, which was connected to ground. $am_7$βCD (Figure S2) was added to the trans compartment (80 μM), which was connected to the head-stage of the amplifier. Both compartments contained 1 M KCl, 25 mM Tris.HCl, at pH 7.5 (0.5 mL). Currents were typically recorded for 5 to 15 min at potentials between +100 to +200 mV. After the addition of $am_7$βCD, transient current

blockades were observed (~70%) (Figure S4). The amplified signal was low-pass filtered at 5 kHz and sampled at 25 kHz with a computer equipped with a Digidata 1440A digitizer (Molecular Devices). The data were analyzed and presented by using pClamp software (version 10.1, Molecular Devices). Events were detected with the 'Event Detection' feature from which current amplitude ($I_B$) and dwell time ($\tau_{off}$) histograms were constructed. The mean $I_B$ value for each base interacting with $am_7\beta CD$ within the αHL pore was determined by performing a Gaussian fit to the histogram of $I_B$ values. The current blockade for each base was also described by a residual current ($I_{RES\%}$), in which $I_B$ is expressed as a percentage of the ionic current with $am_7\beta CD$ bound ($I_{CD}$): $I_{RES\%} = (I_B/I_{CD}) \times 100$. When these experiments were repeated, the rNDPs were added to the chamber in a different order. To determine how well a particular pore can discriminate between rNDPs, two additional criteria were used: (i) the overall dispersion ($\Delta I_{RES\%}{}^{OVERALL}$) was measured (the difference between the most widely separated $I_{RES\%}$ values in the histogram); (ii) the product (δ) of the sequential differences between each of the $I_{RES\%}$[7, 8]. An αHL pore that is unable to discriminate between all four nucleotides has $\delta = 0$.

**rNDP identification by a permanent adapter.** For the continuous detection of rNDPs, we used an αHL pore, αHL-$(N139Q)_6(N139Q/L135C)_1$.$am_6$-$amPDP_1$-βCD, with a covalently attached cyclodextrin. The modified pore was added to the cis compartment. 3 major current levels were observed upon insertion of the pores into the lipid bilayer (Figure S12): (i) 30% of the pores contained no CD; (ii) 10% of the pores gave noisy baselines with currents approaching 0 pA; (iii) 60% were judged to be correctly constructed pores. The latter were characterized by a lower current value (~50% less) than what was seen for the (i) case, due to the presence of the CD. Here, the current remained constant, and the pore was not closed or

removed by changing the polarity or magnitude of the applied potential. Only these pores were used for the identification of rNDPs.

**Detection of rNDP derived from ssRNA.** A 1:1 ratio of *Caulobacter crescentus* PNPase trimer and ssRNA homopolymers: oligo$(rC)_{30}$, oligo$(rU)_{30}$, oligo$(rA)_{30}$ or ssRNA heteropolymer, oligo$(het)_{30}$, obtained from Integrated DNA Technologies (Table S8) were added to the cis compartment. After the addition of 5 mM $MgCl_2$ and 10 mM $NaH_2PO_4$ (pH 7.0), the PNPase was activated and sequentially cleaved rNDPs from the 3'-end of the ssRNA. The liberated rNDPs were observed as binding events when 80 μM $am_7\beta CD$ was added to the trans compartment.

**Monitoring of PNPase digestion.** A 1:1 ratio of *Caulobacter crescentus* PNPase trimer[4] and ssRNA oligonucleotides PNPase•oligo-[P]$(het_{30})$ or oligo-[PS]$(het)_{30}$) obtained from Integrated DNA technologies (Table S8) were added to the cis compartment. After the addition of 5 mM $MgCl_2$ and 10 mM $NaH_2PO_4$ (pH 7.0), the PNPase was activated and sequentially cleaved rNDPs from the 3'-end of the ssRNA. The translocation-event frequency was monitored by collecting capture events in a 30 s segment (from t= 0 s to 900 s), in the presence of $P_i$ and $Mg^{2+}$.

**Supporting Tables and Figures**

| Nucleotide | M113R-RL2 (+120 mV) | | | | | | αHL-(N139Q)$_6$(N139Q/L135C)$_1$.am$_6$-amPDP$_1$-βCD (+160 mV) | | |
|---|---|---|---|---|---|---|---|---|---|
| | am$_7$βCD | | | gu$_7$βCD | | | | | |
| | $\tau_{off}$ (ms) | $k_{off}$ ($s^{-1}$) | $I_{RES}$ (%) | $\tau_{off}$ (ms) | $k_{off}$ ($s^{-1}$) | $I_{RES}$ (%) | $\tau_{off}$ (ms) | $k_{off}$ ($s^{-1}$) | $I_{RES}$ (%) |
| rGMP | 7.0 ±1.0 | 143.0 ±8.0 | 34.3 ±1.2 | 8.0 ±2.0 | 125.0 ±7.0 | 31.4 ±1.4 | 31.0 ±2.0 | 32.0 ±3.0 | 32.7 ±0.4 |
| rAMP | 14.0 ±1.0 | 71.0 ±3.0 | 33.1 ±1.2 | 23.0 ±2.0 | 44.0 ±3.0 | 30.8 ±1.4 | 20.0 ±3.0 | 50.0 ±2.0 | 35.6 ±0.2 |
| rCMP | 11.0 ±2.0 | 91.0 ±7.0 | 37.1 ±1.2 | 18.0 ±1.0 | 55.0 ±3.0 | 32.1 ±1.2 | 24.0 ±2.0 | 41.0 ±1.0 | 36.1 ±0.4 |
| rUMP | 6.0 ±1.0 | 166.0 ±8.0 | 32.6 ±1.6 | 8.0 ±1.0 | 125 ±4.0 | 29.3 ±1.2 | 17.0 ±2.0 | 59.0 ±3.0 | 38.0 ±0.4 |
| $\Delta I_{RES}^{OVERALL}$(%) | 2.5 ±0.3 | | | 4.8 ±0.3 | | | 5.3 ±0.6 | | |
| δ | 1.7 ±0.8 | | | 0.63 ±0.2 | | | 2.8 ±0.4 | | |

**Table S1.** Kinetic parameters for rNMP identification. Comparison of the kinetic parameters of optimal nucleoside monophosphate binding to am$_7$βCD and gu$_7$βCD within the M113R-RL2 αHL mutant pore at pH 6.0 (+120 mV) and to the covalent αHL-(N139Q)$_6$(N139Q/L135C)$_1$.am$_6$-amPDP$_1$-βCD pore at pH 7.5 (+160 mV). Values of $k_{off}$ were determined by using $k_{off} = 1/\tau_{off}$, where $\tau_{off}$ is the mean dwell time of each rNMP in the pore. $I_O$ and $I_{RES\%}$ values are mean values (±S.D.) taken from Gaussian fits to event histograms. $I_{RES\%} = (I_{RES}/I_O) \times 100$. $\Delta I_{RES\%}^{OVERALL}$ is the difference in residual current between the two most widely separated current peaks. δ is the product of the successive differences in $I_{RES\%}$ between the four peaks. If any two peaks overlap, then δ is zero.

| M113X-RL2 mutants | n | **$am_7\beta CD$** | | |
|---|---|---|---|---|
| | | $k_{on}$ | $k_{off}$ | $K_D$ |
| | | $M^{-1}s^{-1}$ | $s^{-1}$ | M |
| M113R | 47 | $2.5 \pm 0.4 \times 10^{5}$ | $3.7 \pm 0.4 \times 10^{3}$ | $1.5 \pm 0.4 \times 10^{-2}$ |
| M113F | 9 | $1.9 \pm 0.6 \times 10^{5}$ | $8.6 \pm 0.6 \times 10^{-2}$ | $4.5 \pm 0.4 \times 10^{-7}$ |
| M113N | 6 | $2.3 \pm 0.4 \times 10^{5}$ | $4.2 \pm 0.2 \times 10^{-2}$ | $1.8 \pm 0.1 \times 10^{-7}$ |

**Table S2.** Kinetic parameters for the interaction of $am_7\beta CD$ with homo-heptameric M113X mutant pores. $k_{on} = 1/\tau_{on}[am_7\beta CD]$, where $\tau_{on}$ is the mean inter-event interval. $k_{off} = 1/\tau_{off}$, where $\tau_{off}$ is the mean dwell time of $am_7\beta CD$ in the pore. $K_D = k_{off}/k_{on}$. n = number of experiments.

| M113R-RL2•am$_7$βCD at +120mV | | | | | | | |
|---|---|---|---|---|---|---|---|
| **Exp** | $I_O$ | rADP | rCDP | rGDP | rUDP | $\Delta I_{RES}^{OVERALL}$ | δ |
| | | $I_{RES}$ | $I_{RES}$ | $I_{RES}$ | $I_{RES}$ | | |
| | (pA) | (%) | (%) | (%) | (%) | (%) | |
| 1 | 121 | 21.4 | 23.1 | 22.0 | 19.2 | 3.9 | 1.5 |
| 2 | 120 | 22.1 | 24.5 | 23.0 | 21.0 | 3.5 | 1.5 |
| 3 | 129 | 21.4 | 24.6 | 24.0 | 20.4 | 4.2 | 1.6 |
| 4 | 120 | 22.0 | 25.1 | 22.8 | 21.1 | 4.0 | 1.7 |
| 5 | 123 | 21.9 | 24.1 | 23.1 | 20.7 | 3.4 | 1.4 |
| **Mean** | 123 | 21.8 | 24.3 | 23.0 | 20.5 | 3.8 | 1.5 |
| **+SD** | 4.0 | 0.3 | 0.7 | 0.7 | 0.8 | 0.3 | 0.1 |

**Table S3.** Reproducibility of rNDP identification at +120 mV with M113R RL2•am$_7$βCD αHL pores. The $I_O$ and $I_{RES\%}$ values are mean values taken from Gaussian fits to event histograms. $I_{RES\%} = (I_{RES}/I_O) \times 100$. $\Delta I_{RES\%}^{OVERALL}$ is the difference in residual current between the two most widely separated current peaks. The δ value is the product of the successive differences between the peaks. If any two peaks overlap, the δ value is zero. The $I_{RES\%}$ values highlighted in grey are plotted as a histogram in Figure 2b.

| Nucleotide | Potential | $\tau_{off}$ | $k_{off}= 1/ \tau_{off}$ | $I_{RES}$ |
|---|---|---|---|---|
| | mV | ms | $s^{-1}$ | (%) |
| **rGDP** | 100 | 24.0 ±2.0 | 42.0 ±1.0 | 20.4 ±1.4 |
| | 120 | 24.0 ±1.0 | 41.0 ±2.0 | 23.0 ±0.7 |
| | 140 | 26.0 ±3.0 | 39.0 ±1.0 | 26.1 ±2.0 |
| | 160 | 27.0 ±1.6 | 37.0 ±1.0 | 30.6 ±1.4 |
| | 180 | 28.0 ±1.0 | 37.0 ±2.0 | 35.8 ±2.0 |
| | 200 | 30.0 ±2.0 | 36.0 ±1.0 | 40.1 ±1.6 |
| **rADP** | 100 | 21.0 ±1.0 | 48.0 ±1.0 | 18.1 ±1.4 |
| | 120 | 23.0 ±2.0 | 43.0 ±1.0 | 21.8 ±0.3 |
| | 140 | 24.0 ±2.0 | 42.0 ±1.0 | 25.9 ±1.4 |
| | 160 | 27.0 ±1.0 | 37.0 ±4.0 | 30.0 ±1.4 |
| | 180 | 26.0 ±1.0 | 39.0 ±4.0 | 33.8 ±2.0 |
| | 200 | 27.0 ±2.0 | 37.0 ±4.0 | 39.5 ±2.0 |

| Nucleotide | Potential | $\tau_{off}$ | $k_{off}= 1/\tau_{off}$ | $I_{RES}$ |
|---|---|---|---|---|
| | mV | ms | $s^{-1}$ | (%) |
| **rCDP** | 100 | 19.0 ±2.0 | 54.0 ±2.0 | 21.7 ±0.7 |
| | 120 | 20.0 ±2.0 | 50.0 ±2.0 | 24.3 ±0.7 |
| | 140 | 22.0 ±1.0 | 46.0 ±1.0 | 28.0 ±1.6 |
| | 160 | 23.0 ±3.0 | 44.0 ±1.0 | 31.6 ±1.6 |
| | 180 | 22.0 ±1.0 | 45.0 ±1.0 | 36.0 ±1.4 |
| | 200 | 22.0 ±2.0 | 46.0 ±1.0 | 40.6 ±2.0 |
| **rUDP** | 100 | 25.0 ±2.0 | 40.0 ±2.0 | 16.0 ±2.0 |
| | 120 | 27.0 ±1.0 | 37.0 ±2.0 | 20.5 ±0.8 |
| | 140 | 29.0 ±1.0 | 34.0 ±2.0 | 24.1 ±2.0 |
| | 160 | 31.0 ±2.0 | 32.0 ±2.0 | 28.6 ±2.0 |
| | 180 | 30.0 ±1.0 | 33.0 ±2.0 | 32.4 ±2.0 |
| | 200 | 28.0 ±2.0 | 35.0 ±2.0 | 38.3 ±2.0 |

**Table S4.** Voltage dependences of the residual currents ($I_{RES\%}$), dwell times ($\tau_{off}$) and dissociation rate constants ($k_{off} = 1/\tau_{off}$) for rNDP bound to the M113R-RL2•$am_7\beta$CD αHL pore. $I_{RES\%}$ values are mean values (± S.D.) taken from Gaussian fits to event histograms at various applied potentials ($n \geq 3$ experiments). $I_{RES\%} = (I_{RES}/I_O) \times 100$. Plots of applied potential versus $I_{RES\%}$ and $k_{off}$ are shown in Figures 2c-d.

| | M113R-RL2 at +120mV | | | | | |
|---|---|---|---|---|---|---|
| | **$am_7\beta CD$** | | | **$gu_7\beta CD$** | | |
| Nucleotide | $\tau_{off}$ | $k_{off}= 1/\tau_{off}$ | $I_{RES}$ | $\tau_{off}$ | $k_{off}= 1/\tau_{off}$ | $I_{RES}$ |
| | ms | $s^{-1}$ | (%) | ms | $s^{-1}$ | (%) |
| rGDP | 11.0 ±1.0 | 91.0 ±4.0 | 23.1 ±0.7 | 16.0 ±1.2 | 43.0 ±6.0 | 25.6 ±1.2 |
| rADP | 20.0 ±1.6 | 50.0 ±6.0 | 21.9 ±0.3 | 21.0 ±1.1 | 46.0 ±6.0 | 23.0 ±1.2 |
| rCDP | 16.0 ±2.0 | 63.0 ±2.0 | 24.1 ±0.7 | 16.0 ±1.2 | 42.0 ±8.0 | 26.4 ±1.6 |
| rUDP | 9.0 ±1.0 | 111.0 ±6.0 | 20.7 ±0.8 | 11.0 ±1.0 | 49.0 ±6.0 | 22.1 ±2.0 |
| | $\Delta I_{RES}^{OVERALL}$ (%) | | 3.4 ±0.3 | $\Delta I_{RES}^{OVERALL}$ (%) | | 4.3 ±0.4 |
| | δ | | 1.4 ±0.6 | δ | | 1.9 ±0.4 |

**Table S5.** Comparison of kinetic parameters for rNDP binding to $am_7\beta CD$ and $gu_7\beta CD$ in αHL M113R-RL2 αHL pores at pH 6.0 (+120 mV). $k_{on} = 1/\tau_{on}$ [$am_7\beta CD$], where $\tau_{on}$ is the mean inter-event interval. $k_{off} = 1/\tau_{off}$, where $\tau_{off}$ is the mean dwell time of $am_7\beta CD$ in the pore. $I_O$ and $I_{RES\%}$ values are mean values (±S.D.) taken from Gaussian fits to event histograms. $I_{RES\%} = (I_{RES}/I_O) \times 100$. $\Delta I_{RES\%}^{OVERALL}$ is the difference in residual current between the two most widely separated current peaks. The δ value is the product of the successive differences between the peaks. If any two peaks overlap, then the δ value is zero.

| αHL-$(N139Q)_6(N139Q/L135C)_1$.$am_6$-$amPDP_1$-βCD at +160mV | | | | | | | |
|---|---|---|---|---|---|---|---|
| **Exp** | $I_O$ | rADP | rCDP | rGDP | rUDP | $\Delta I_{RES}^{OVERALL}$ | δ |
| | | $I_{RES}$ | $I_{RES}$ | $I_{RES}$ | $I_{RES}$ | | |
| | (pA) | (%) | (%) | (%) | (%) | (%) | |
| 1 | 70 | 29.4 | 31.8 | 28.0 | 32.6 | 4.6 | 2.7 |
| 2 | 67 | 29.5 | 31.6 | 27.9 | 33.0 | 5.1 | 4.7 |
| 3 | 69 | 28.9 | 31.4 | 28.2 | 32.6 | 4.4 | 2.1 |
| 4 | 79 | 29.8 | 32.1 | 28.1 | 33.0 | 4.9 | 3.5 |
| 5 | 72 | 29.5 | 31.8 | 27.7 | 32.4 | 4.7 | 2.5 |
| **Mean** | 71 | 29.4 | 31.7 | 28.0 | 32.7 | 4.7 | 3.1 |
| **±SD** | 5.0 | 0.3 | 0.3 | 0.2 | 0.3 | 0.3 | 1.0 |

**Table S6.** Reproducibility of rNDP identification at +160 mV with αHL-$(N139Q)_6(N139Q/L135C)_1$.$am_6$-$amPDP_1$-βCD pores. $I_O$ and $I_{RES\%}$ are mean values (±S.D.) taken from Gaussian fits to event histograms. $I_{RES\%} = (I_{RES}/I_O) \times 100$. $\Delta I_{RES\%}^{OVERALL}$ is the difference in residual current between the two most widely separated current peaks. The δ value is the product of the successive differences between the peaks. If any two peaks overlap, then the δ value is zero. The $I_{RES\%}$ values highlighted in grey are plotted as a histogram in Figure 3c.

| Nucleotide | Potential | $\tau_{off}$ | $k_{off}= 1/\tau_{off}$ | $I_{RES}$ |
|---|---|---|---|---|
| | mV | ms | $s^{-1}$ | (%) |
| **rGDP** | 100 | 20.0 ±1.0 | 49.0 ±1.0 | 16.5 ±1.0 |
| | 120 | 22.0 ±2.0 | 45.0 ±1.0 | 21.2 ±0.8 |
| | 140 | 25.0 ±2.0 | 41.0 ±1.0 | 24.6 ±0.8 |
| | 160 | 26.0 ±2.0 | 38.0 ±1.0 | 28.0 ±0.2 |
| | 180 | 27.0 ±1.0 | 39.0 ±1.0 | 29.2 ±0.4 |
| | 200 | 23.0 ±2.0 | 43.0 ±1.0 | 34.2 ±0.6 |
| **rADP** | 100 | 16.0 ±1.0 | 62.0 ±1.0 | 17.2 ±0.6 |
| | 120 | 18.0 ±1.0 | 55.0 ±1.0 | 22.1 ±0.4 |
| | 140 | 19.0 ±1.0 | 50.0 ±1.0 | 26.0 ±0.8 |
| | 160 | 22.0 ±2.0 | 46.0 ±1.0 | 29.4 ±0.3 |
| | 180 | 21.0 ±1.0 | 48.0 ±1.0 | 33.3 ±0.8 |
| | 200 | 22.0 ±1.0 | 45.0 ±1.0 | 38.2 ±0.8 |

| Nucleotide | Potential | $\tau_{off}$ | $k_{off}= 1/\tau_{off}$ | $I_{RES}$ |
|---|---|---|---|---|
| | mV | ms | $s^{-1}$ | (%) |
| **rCDP** | 100 | 19.0 ±1.0 | 53.0 ±1.0 | 18.5 ±0.6 |
| | 120 | 20.0 ±1.0 | 51.0 ±1.0 | 25.2 ±0.4 |
| | 140 | 21.0 ±1.0 | 48.0 ±1.0 | 29.1 ±0.4 |
| | 160 | 23.0 ±2.0 | 44.0 ±1.0 | 31.7 ±0.3 |
| | 180 | 22.0 ±1.0 | 45.0 ±1.0 | 34.8 ±1.2 |
| | 200 | 23.0 ±2.0 | 43.0 ±1.0 | 41.1 ±1.0 |
| **rUDP** | 100 | 14.0 ±2.0 | 73.0 ±1.0 | 18.7 ±0.4 |
| | 120 | 15.0 ±1.0 | 66.0 ±1.0 | 23.7 ±1.0 |
| | 140 | 17.0 ±2.0 | 59.0 ±1.0 | 28.5 ±1.0 |
| | 160 | 18.0 ±3.0 | 57.0 ±1.0 | 32.7 ±0.3 |
| | 180 | 17.0 ±1.0 | 58.0 ±1.0 | 36.0 ±0.2 |
| | 200 | 16.0 ±2.0 | 60.0 ±1.0 | 39.7 ±0.6 |

**Table S7.** Voltage dependences of the residual currents ($I_{RES\%}$), mean dwell times ($\tau_{off}$) and dissociation rate constants ($k_{off} = 1/\tau_{off}$) for rNDPs bound to the αHL-$(N139Q)_6(N139Q/L135C)_1$.$am_6$-$amPDP_1$-βCD pore. $I_{RES\%}$ values are mean values (± S.D.) taken from Gaussian fits to event histograms at various applied potentials ($n \geq 3$ experiments). $I_{RES\%} = (I_{RES}/I_O) \times 100$. Plots of applied potential versus $I_{RES\%}$ and $k_{off}$ are shown in Figures 3e-f.

| Oligonucleotide name | Oligonucleotide sequence (3'→5') |
|---|---|
| oligo(rA)$_{30}$ | 3'-AAAAAAAAAAAAAAAAAAAAAAAAAAAAAA-5' |
| oligo(rC)$_{30}$ | 3'-CCCCCCCCCCCCCCCCCCCCCCCCCCCCCC-5' |
| oligo(rU)$_{30}$ | 3'-UUUUUUUUUUUUUUUUUUUUUUUUUUUUUU-5' |
| oligo-(het)$_{30}$ | 3'-AAAUGGACUGGCUUCGGAAGCCAAAUGGAU-5' |
| oligo-[P](het)$_{30}$ | 3'-[P]AAAUGGACUGGCUUCGGAAGCCAAAUGGAU-5' |
| oligo-[PS](het)$_{30}$ | 3'- [PS]AAAUGGACUGGCUUCGGAAGCCAAAUGGAU-5' |

**Table S8.** Sequences of the oligonucleotides used in this study. (het) represents the heteropolymer oligonucleotide consisting of all four nucleotides (rC, rG, rA and rU). [P] represents the phosphodiester linkage and [PS] represents a 3'-phosphorylated linkage in the oligonucleotide backbone.

| M113R-RL2 | | | | | M113R-RL2•am$_7$βCD | | | | | |
|---|---|---|---|---|---|---|---|---|---|---|
| **Exp** | $I_O$ | oligo(rA)$_{30}$ | oligo(rC)$_{30}$ | oligo(rU)$_{30}$ | rADP | | rCDP | | rUDP | |
| | | $I_{RES}$ | $I_{RES}$ | $I_{RES}$ | $I_{RES}$ | $\tau_{off}$ | $I_{RES}$ | $\tau_{off}$ | $I_{RES}$ | $\tau_{off}$ |
| | (pA) | (%) | (%) | (%) | (%) | ms | (%) | ms | (%) | ms |
| 1 | 140 | 24.0 | 26.6 | 21.9 | 29.7 | 19.0 | 32.1 | 20.0 | 28.1 | 18.0 |
| 2 | 142 | 24.5 | 26.5 | 22.2 | 29.6 | 19.0 | 31 | 20.0 | 27 | 16.0 |
| 3 | 141 | 23.3 | 25.4 | 21.3 | 26.8 | 17.0 | 29.7 | 19.0 | 25.9 | 16.0 |
| 4 | 136 | 24.2 | 26.7 | 22.0 | 28.2 | 19.0 | 31.6 | 21.0 | 26.1 | 18.0 |
| 5 | 138 | 24.3 | 26.7 | 22.4 | 28.1 | 19.0 | 30.7 | 20.0 | 26.9 | 16.0 |
| 6 | 141 | 23.9 | 26.9 | 22.6 | 27.9 | 18.0 | 30.8 | 21.0 | 27.6 | 18.0 |
| 7 | 139 | 24.5 | 26.4 | 22.0 | 29.9 | 19.0 | 31.9 | 20.0 | 26 | 16.0 |
| 8 | 142 | 24.3 | 26.6 | 22.2 | 28.8 | 20.0 | 31.3 | 21.0 | 26.9 | 18.0 |
| **Mean** | 140 | 24.1 | 26.5 | 22.1 | 28.6 | 19.0 | 31.1 | 20.0 | 26.8 | 17.0 |
| **±SD** | 2.0 | 0.4 | 0.5 | 0.4 | 1.1 | 1.0 | 0.8 | 1.0 | 0.8 | 1.0 |

**Table S9.** Reproducibility of experiments with PNPase•RNA complexes captured using the voltage protocol described in Figure S9. The rNDPs liberated by the PNPase enzyme (in the presence of $P_i$ and $Mg^{2+}$) are detected by M113R-RL2•am$_7$βCD αHL pores at +140 mV. The $I_O$ and $I_{RES\%}$ values are mean values (±S.D.) taken from Gaussian fits to event histograms. $I_{RES\%} = (I_{RES}/I_O) \times 100$. $\Delta I_{RES\%}^{OVERALL}$ is the difference in residual current between the two most widely separated current peaks. The δ value is the product of the successive differences between the peaks. If any two peaks overlap, then the δ value is zero. The $I_{RES\%}$ values highlighted in grey are plotted as histograms in Figure 4c-d.

| $I_{RES\%}$ values for PNPase•oligo(het)$_{30}$ and released rNDPs | | | | | | | | | | | | |
|---|---|---|---|---|---|---|---|---|---|---|---|---|
| **Exp** | $I_O$ | oligo(het)$_{30}$ | rADP | | rCDP | | rGDP | | rUDP | | $\Delta I_{RES}^{OVERALL}$ | δ |
| | | $I_{RES}$ | $I_{RES}$ | $\tau_{off}$ | $I_{RES}$ | $\tau_{off}$ | $I_{RES}$ | $\tau_{off}$ | $I_{RES}$ | $\tau_{off}$ | | |
| | (pA) | (%) | % | ms | (%) | ms | (%) | ms | (%) | ms | (%) | |
| 1 | 140 | 24.6 | 26.4 | 20.0 | 30.4 | 22.0 | 27.2 | 27.0 | 25.9 | 18.0 | 4.5 | 1.3 |
| 2 | 143 | 25.6 | 26.1 | 17.0 | 28.3 | 19.0 | 26.6 | 23.0 | 25.5 | 15.0 | 2.8 | 0.5 |
| 3 | 141 | 25.1 | 27.2 | 20.0 | 30.1 | 21.0 | 29.4 | 25.0 | 26.1 | 17.0 | 4.0 | 1.7 |
| 4 | 146 | 25.3 | 27.1 | 16.0 | 28.4 | 18.0 | 27.6 | 21.0 | 23.9 | 15.0 | 4.5 | 1.3 |
| 5 | 137 | 25.2 | 27.1 | 19.0 | 29.9 | 21.0 | 28.2 | 25.0 | 25.8 | 17.0 | 4.1 | 2.4 |
| **Mean** | 141 | 25.2 | 26.8 | 18.0 | 29.4 | 20.0 | 27.8 | 24.0 | 25.4 | 16.0 | 4.0 | 1.4 |
| **±SD** | 3.0 | 0.4 | 0.5 | 2.0 | 1.0 | 2.0 | 1.1 | 2.0 | 0.9 | 1.0 | 0.7 | 0.7 |

**Table S10.** Reproducibility of experiments with captured PNPase•oligo(het)$_{30}$ complexes and released rNDP binding events with αHL M113R RL2•am$_7$βCD pores. The voltage protocol is described in Figure S9. The rNDPs were cleaved by PNPase from the RNA oligo(het)$_{30}$ and detected with αHL M113R RL2•am$_7$βCD at +140 mV. The $I_O$ and $I_{RES\%}$ values are mean values (±S.D.) taken from Gaussian fits to event histograms. $I_{RES\%} = (I_{RES}/I_O) \times 100$. $\tau_{off}$ is the mean dwell time of a rNDP in the pore. $\Delta I_{RES\%}^{OVERALL}$ is the difference in residual current between the two most widely separated current peaks. The δ value is the product of the successive differences between the peaks. If any two peaks overlap, then the δ value is zero. The $I_{RES\%}$ values highlighted in grey are plotted as histograms in Figure 4e-f.

| Time (s) | # Events | | | | | | | | | | | | | | |
|---|---|---|---|---|---|---|---|---|---|---|---|---|---|---|---|
| | oligo-[P](het)$_{30}$ | | | | | oligo-[PS](het)$_{30}$ | | | | | Control, oligo-[P](het)$_{30}$ (no Pi) | | | | |
| | #1 | #2 | #3 | Mean | ±S.D | #1 | #2 | #3 | Mean | ±S.D | #1 | #2 | #3 | Mean | ±S.D |
| 0 | 36 | 42 | 46 | 41 | 5 | 46 | 42 | 38 | 42 | 4 | 44 | 38 | 44 | 42 | 3 |
| 30 | 37 | 38 | 51 | 42 | 8 | 44 | 38 | 34 | 39 | 5 | 40 | 41 | 46 | 42 | 3 |
| 60 | 41 | 41 | 44 | 42 | 2 | 41 | 39 | 39 | 40 | 1 | 41 | 44 | 41 | 42 | 2 |
| 90 | 39 | 38 | 41 | 39 | 2 | 42 | 42 | 41 | 42 | 1 | 44 | 37 | 49 | 43 | 6 |
| 120 | 35 | 32 | 37 | 35 | 3 | 48 | 45 | 46 | 46 | 2 | 47 | 46 | 49 | 47 | 2 |
| 150 | 37 | 46 | 41 | 41 | 5 | 41 | 48 | 42 | 44 | 4 | 50 | 47 | 47 | 48 | 2 |
| 180 | 38 | 47 | 41 | 42 | 5 | 40 | 44 | 44 | 43 | 2 | 46 | 41 | 41 | 43 | 3 |
| 210 | 34 | 37 | 33 | 35 | 2 | 37 | 46 | 49 | 44 | 6 | 48 | 42 | 42 | 44 | 3 |
| 240 | 41 | 41 | 42 | 41 | 1 | 39 | 46 | 47 | 44 | 4 | 48 | 54 | 46 | 49 | 4 |
| 270 | 37 | 46 | 41 | 41 | 5 | 39 | 42 | 39 | 40 | 2 | 44 | 52 | 55 | 50 | 6 |
| 300 | 36 | 42 | 31 | 36 | 6 | 44 | 41 | 37 | 41 | 4 | 43 | 46 | 56 | 48 | 7 |
| 330 | 41 | 36 | 40 | 39 | 3 | 37 | 47 | 34 | 39 | 7 | 49 | 43 | 51 | 48 | 4 |
| 360 | 45 | 44 | 45 | 45 | 1 | 43 | 49 | 46 | 46 | 3 | 51 | 40 | 49 | 47 | 6 |
| 390 | 40 | 34 | 41 | 38 | 4 | 42 | 40 | 42 | 41 | 1 | 42 | 47 | 59 | 49 | 9 |
| 420 | 43 | 37 | 40 | 40 | 3 | 38 | 39 | 34 | 37 | 3 | 41 | 46 | 44 | 44 | 3 |
| 450 | 35 | 23 | 37 | 32 | 8 | 39 | 39 | 46 | 41 | 4 | 41 | 42 | 41 | 41 | 1 |
| 480 | 29 | 21 | 27 | 26 | 4 | 42 | 49 | 41 | 44 | 4 | 51 | 41 | 42 | 45 | 6 |
| 510 | 22 | 25 | 21 | 23 | 2 | 46 | 50 | 40 | 45 | 5 | 52 | 43 | 41 | 45 | 6 |
| 540 | 27 | 22 | 21 | 23 | 3 | 40 | 47 | 40 | 42 | 4 | 49 | 44 | 43 | 45 | 3 |
| 570 | 24 | 24 | 13 | 20 | 6 | 37 | 49 | 49 | 45 | 7 | 51 | 41 | 46 | 46 | 5 |
| 600 | 20 | 20 | 14 | 18 | 3 | 39 | 46 | 48 | 44 | 5 | 48 | 40 | 52 | 47 | 6 |
| 630 | 21 | 26 | 22 | 23 | 3 | 39 | 42 | 51 | 44 | 6 | 44 | 40 | 44 | 43 | 2 |
| 660 | 13 | 20 | 17 | 17 | 4 | 44 | 43 | 34 | 40 | 6 | 45 | 42 | 40 | 42 | 3 |
| 690 | 6 | 18 | 17 | 14 | 7 | 36 | 49 | 31 | 39 | 9 | 51 | 49 | 49 | 50 | 1 |
| 720 | 2 | 13 | 11 | 9 | 6 | 41 | 47 | 39 | 42 | 4 | 49 | 47 | 38 | 45 | 6 |
| 750 | 1 | 7 | 8 | 5 | 4 | 44 | 42 | 38 | 41 | 3 | 44 | 35 | 40 | 40 | 5 |
| 780 | 0 | 3 | 3 | 2 | 2 | 41 | 46 | 34 | 40 | 6 | 48 | 37 | 37 | 41 | 6 |
| 810 | 0 | 1 | 5 | 2 | 3 | 47 | 42 | 36 | 42 | 6 | 44 | 46 | 46 | 45 | 1 |
| 840 | 0 | 0 | 0 | 0 | 0 | 40 | 41 | 42 | 41 | 1 | 43 | 39 | 43 | 42 | 2 |
| 870 | 0 | 0 | 1 | 0 | 1 | 39 | 49 | 40 | 43 | 6 | 51 | 38 | 47 | 45 | 7 |
| 900 | 0 | 0 | 0 | 0 | 0 | 40 | 44 | 41 | 42 | 2 | 46 | 39 | 42 | 42 | 4 |
| **Total** | 780 | 824 | 831 | 812 | 28 | 1275 | 1373 | 1262 | 1303 | 61 | 1435 | 1327 | 1410 | 1391 | 57 |

**Table S11.** The PNPase•RNA capture rate by the αHL M113R-RL2 nanopore as a function of time. After the addition of 10 mM $P_i$ (at t = 360 s, highlighted in grey), the event rate sharply declines for oligo-[P](het)$_{30}$. In contrast, the event rate is maintained for the phosphorothioate oligonucleotide, oligo-[PS](het)$_{30}$ which cannot be digested by PNPase. In the control experiments with oligo-[P](het)$_{30,}$ $P_i$ is not added. The data are plotted in Figure 5b.

| Time (s) | Digestion % | | | | |
|---|---|---|---|---|---|
| | oligo-[P](het)$_{30}$ | | | | |
| | #1 | #2 | #3 | Mean | ±S.D |
| 0 | 4.6 | 5.1 | 5.5 | 5.1 | 0.5 |
| 30 | 9.4 | 9.7 | 11.7 | 10.2 | 1.2 |
| 60 | 14.6 | 14.7 | 17.0 | 15.4 | 1.3 |
| 90 | 19.6 | 19.3 | 21.9 | 20.3 | 1.4 |
| 120 | 24.1 | 23.2 | 26.4 | 24.5 | 1.6 |
| 150 | 28.8 | 28.8 | 31.3 | 29.6 | 1.4 |
| 180 | 33.7 | 34.5 | 36.2 | 34.8 | 1.3 |
| 210 | 38.1 | 39.0 | 40.2 | 39.1 | 1.1 |
| 240 | 43.3 | 43.9 | 45.2 | 44.2 | 1.0 |
| 270 | 48.1 | 49.5 | 50.2 | 49.3 | 1.1 |
| 300 | 52.7 | 54.6 | 53.9 | 53.7 | 1.0 |
| 330 | 57.9 | 59.0 | 58.7 | 58.6 | 0.5 |
| 360 | 63.7 | 64.3 | 64.1 | 64.1 | 0.3 |
| 390 | 68.8 | 68.4 | 69.1 | 68.8 | 0.3 |
| 420 | 74.4 | 72.9 | 73.9 | 73.7 | 0.7 |
| 450 | 78.8 | 75.7 | 78.3 | 77.6 | 1.7 |
| 480 | 82.6 | 78.3 | 81.6 | 80.8 | 2.2 |
| 510 | 85.4 | 81.3 | 84.1 | 83.6 | 2.1 |
| 540 | 88.8 | 84.0 | 86.6 | 86.5 | 2.4 |
| 570 | 91.9 | 86.9 | 88.2 | 89.0 | 2.6 |
| 600 | 94.5 | 89.3 | 89.9 | 91.2 | 2.8 |
| 630 | 97.2 | 92.5 | 92.5 | 94.1 | 2.7 |
| 660 | 98.8 | 94.9 | 94.6 | 96.1 | 2.4 |
| 690 | 99.6 | 97.1 | 96.6 | 97.8 | 1.6 |
| 720 | 99.9 | 98.7 | 98.0 | 98.8 | 1.0 |
| 750 | 100.0 | 99.5 | 98.9 | 99.5 | 0.5 |
| 780 | 100.0 | 99.9 | 99.3 | 99.7 | 0.4 |
| 810 | 100.0 | 100.0 | 99.9 | 100.0 | 0.1 |
| 840 | 100.0 | 100.0 | 99.9 | 100.0 | 0.1 |
| 870 | 100.0 | 100.0 | 100.0 | 100.0 | 0.0 |
| 900 | 100.0 | 100.0 | 100.0 | 100.0 | 0.0 |

**Table S12.** Time course for the digestion of oligo-[P](het)$_{30}$ with PNPase. To obtain the plot of percent ssRNA digestion versus time (Figure 5c), events were collected in 30-s segments (between 30 to 900 s) from single-channel current traces of αHL M113R-RL2 and PNPase•oligo-[P](het)$_{30,}$ before and after the addition of 10 mM $P_i$ (cis).

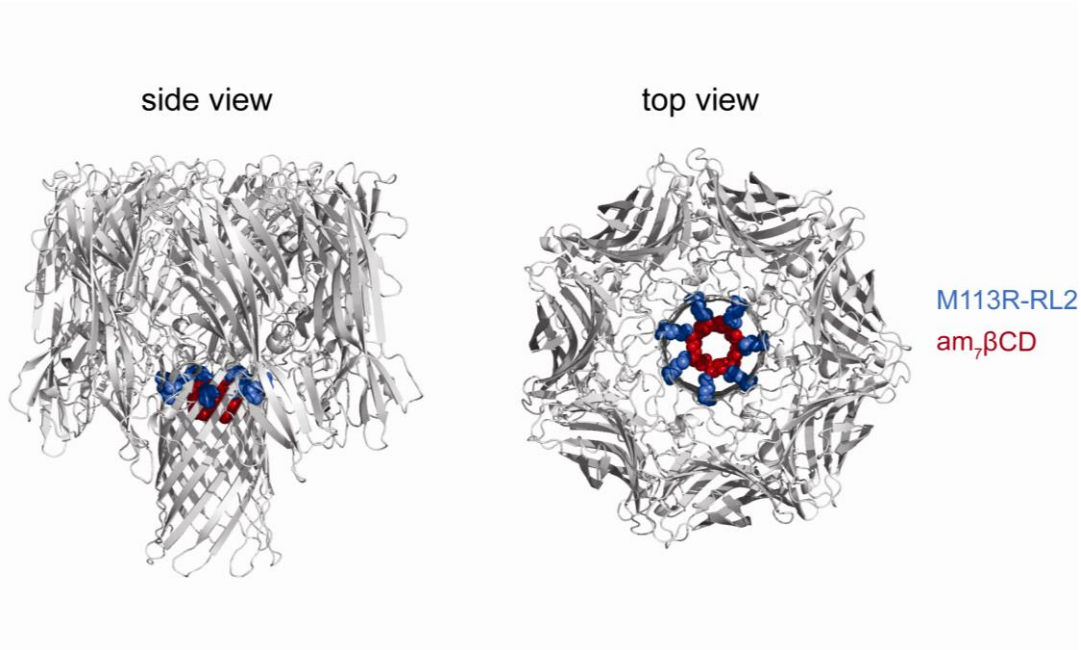


**Figure S1.** Structure of the M113R-RL2 αHL pore (cartoon view). (*Left*) top view; (*Right*), side view. Arg-113 (blue) and the $am_7$βCD cyclodextrin (red) are shown as space-filling structures, Created using PyMOL software (version 1.3).

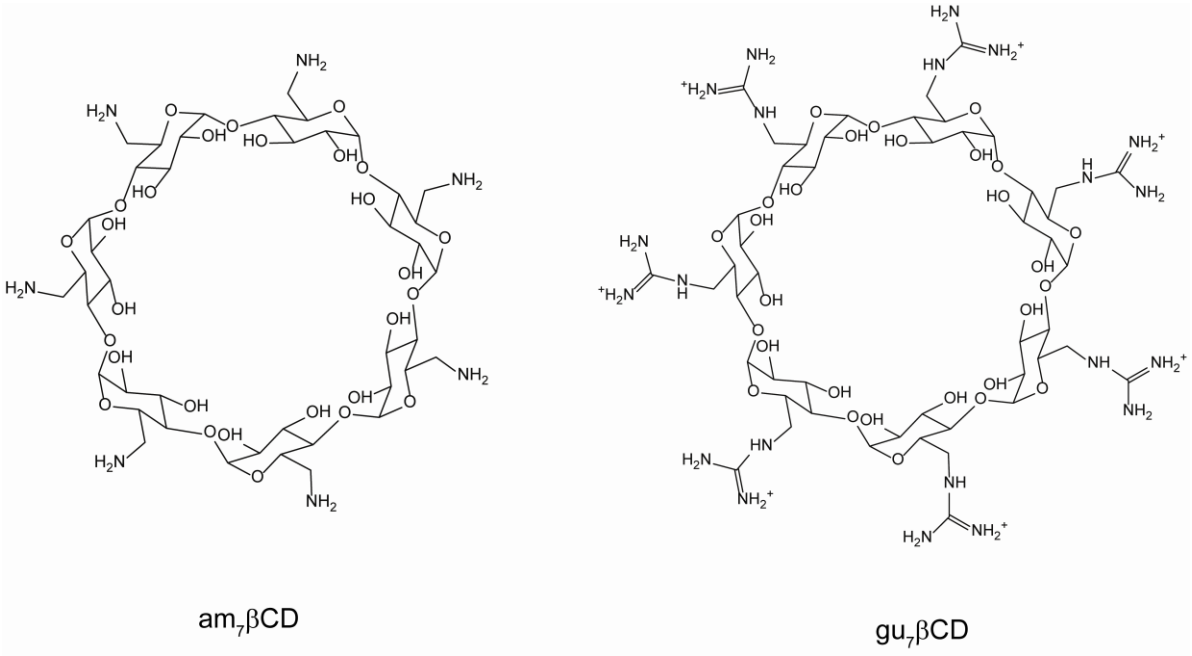


**Figure S2.** Structures of the $am_7\beta CD$ and $gu_7\beta CD$ adapters (ChemBioDraw Ultra software, version 12.02).

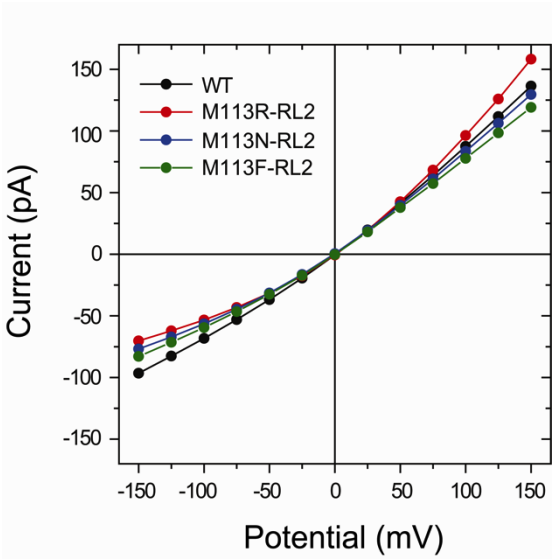


**Figure S3.** Typical current-voltage (I-V) traces for αHL WT (black), αHL M113R-RL2 (red), αHL M113N-RL2 (blue) and αHL M113F-RL2 (green) pores in 1 M KCl, 25 mM Tris-HCl, at pH 6.0.

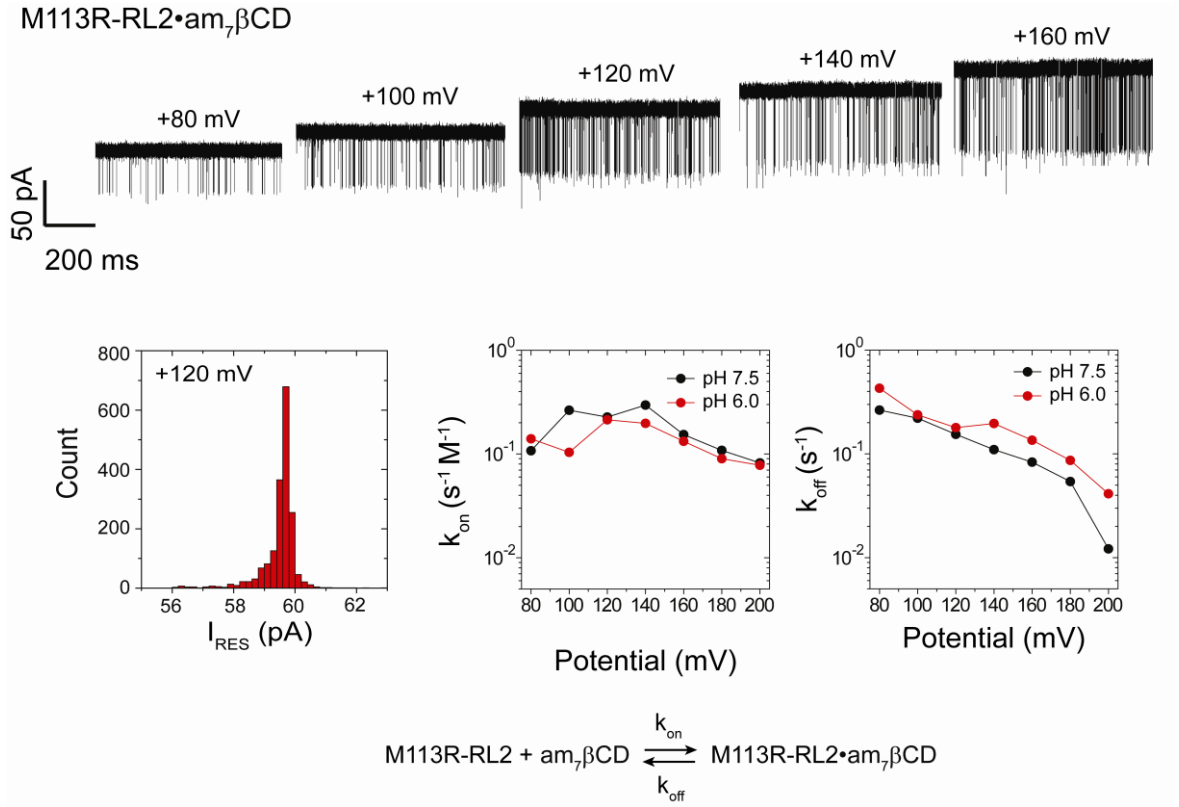


**Figure S4.** $am_7\beta CD$ characterisation in M113R-RL2 pores. (*Top*) Representative single-channel recordings of $am_7\beta CD$ (80 μM) binding inside the αHL M113R-RL2 pore at potentials between +80 mV and +160 mV. The traces were recorded in 1.2 M KCl, 25 mM Tris-HCl, pH 6.0. (*Bottom, left*) Residual current ($I_{RES}$) histogram for $am_7\beta CD$ at +120 mV. (*Bottom, right*) Comparison of the kinetic parameters for the interaction of $am_7\beta CD$ with αHL M113R-RL2 mutant pores at pH 6.0 and 7.5 versus the applied potential. $k_{on} = 1/\tau_{on}[am_7\beta CD]$, where $\tau_{on}$ is the mean inter-event interval. $k_{off} = 1/\tau_{off}$, where $\tau_{off}$ is the mean dwell time of $am_7\beta CD$ within the pore.

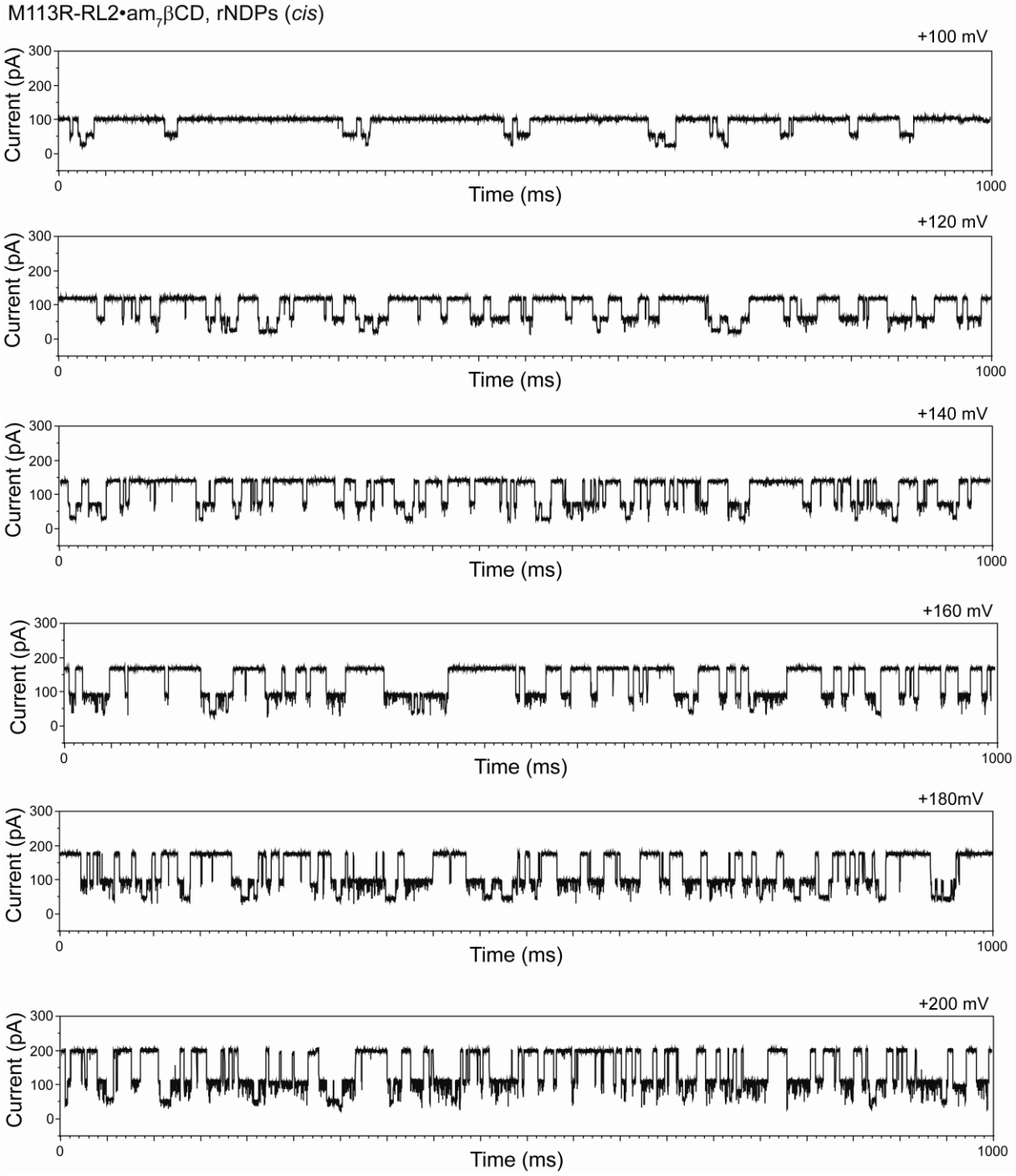


**Figure S5.** Representative single-channel recordings with the αHL M113R-RL2 pore at potentials between +100 mV and +200 mV, showing transient adapter binding (80 μM am-$_7$βCD, trans) and rNDP detection. The traces were recorded in 1.2 M KCl, 25 mM Tris-HCl, at pH 6.0, in the presence of 10 μM rADP, 10 μM rUDP, 10 μM rCDP and 10 μM rGDP (all cis).

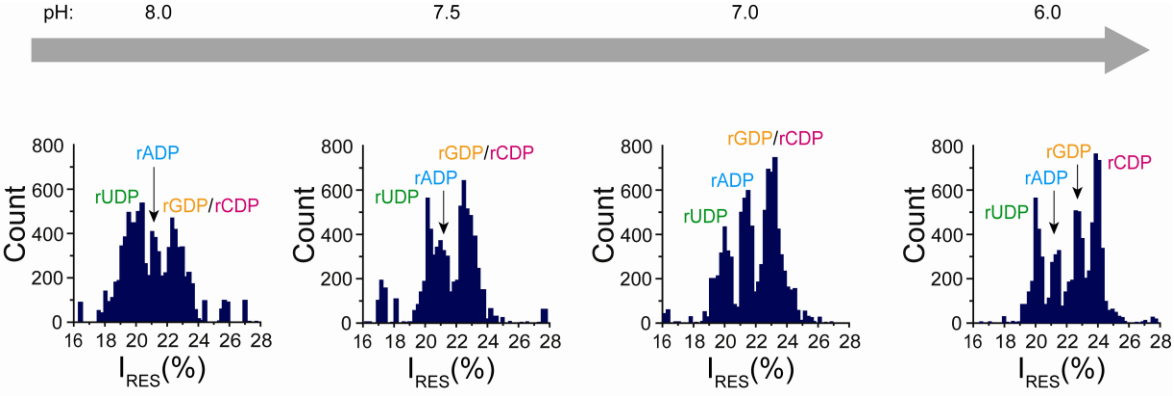


**Figure S6.** pH-dependence of rNDP detection with M113R-RL2•am$_7$βCD αHL pores. Tris-HCl buffers containing 1.2 M KCl at pH values of 6.0, 7.0, 7.5 and 8.0 were examined. Between pH 7.0 and 8.0, only three current levels were observed in the presence of all four rNDPs. At pH 6.0, the four rNDPs could be distinguished.

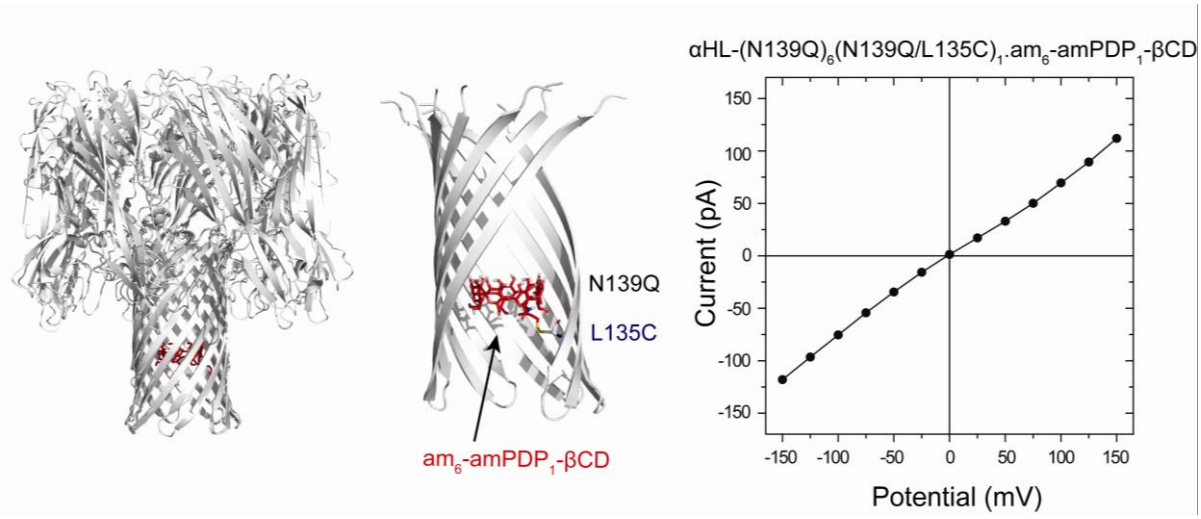


**Figure S7.** Structure of the αHL-$(N139Q)_6(N139Q/L135C)_1$.$am_6$-$amPDP_1$-βCD pore. (*Left*) Full length of the αHL pore (cartoon view). (*Middle*) Enlarged view showing the close-up of the β barrel with two subunits omitted. The cyclodextrin ($am_6$-$amPDP_1$-βCD, red sticks) is covalently attached through a disulfide bond to Cys-135 of the N139Q/L135C subunit. (*Right)* Typical current-voltage (I-V) traces for the αHL-$(N139Q)_6(N139Q/L135C)_1$.$am_6$-$amPDP_1$-βCD mutant in 1 M KCl, 25 mM Tris-HCl, pH 7.5.

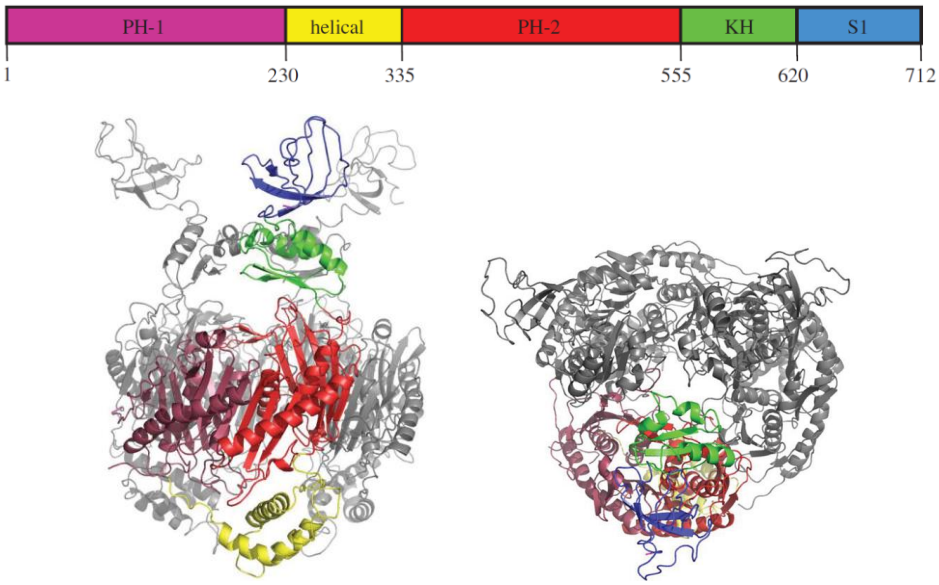


**Figure S8.** The structure of *Caulobacter crescentus* polynucleotide phosphorylase. (a) Linear schematic of domain organization, showing the two RNase PH domains, the helical domain, the KH and S1 RNA-binding domains. (b) Schematic of the structure of the trimeric PNPase. (i) Side view and (ii) perpendicular view along the 3-fold axis. For one of the protomers, the individual sub-domains are colour coded according to the scheme above. The other two protomers are grey. (Adapted from reference[4])

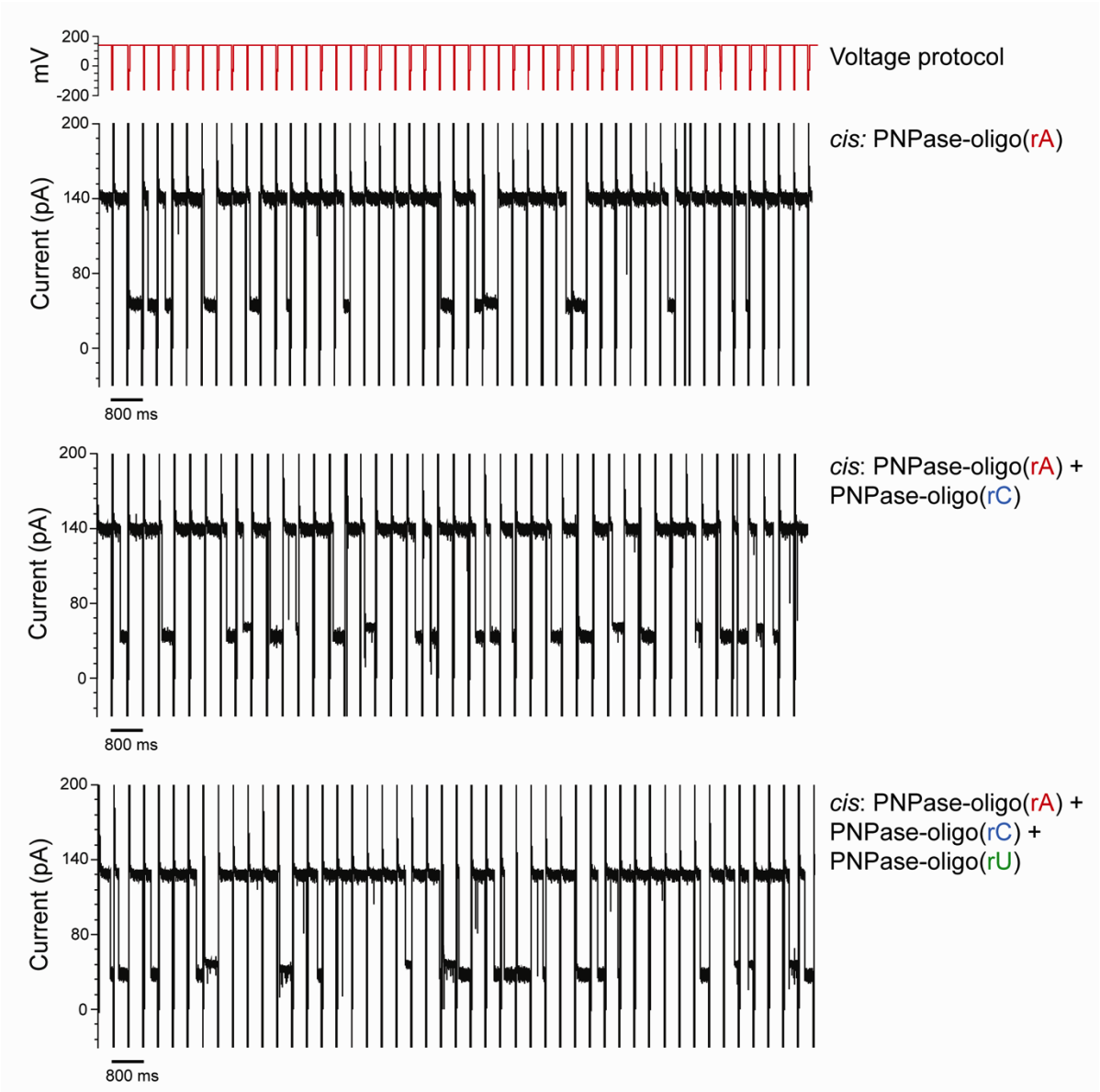


**Figure S9.** The voltage protocol used to capture the PNPase•RNA complexes inside the αHL pore and the corresponding current traces for the complexes with oligo(rA)$_{30}$, oligo(rC)$_{30}$ and oligo(rU)$_{30}$ added sequentially from the cis compartment. A single cycle consists of +140 mV applied to drive a complex into the pore (t= 380 ms), followed by reversal of the potential to -160 mV (20 ms) to expel the complex Current traces and histograms of the data from these experiments are shown in Figure 4b-c.

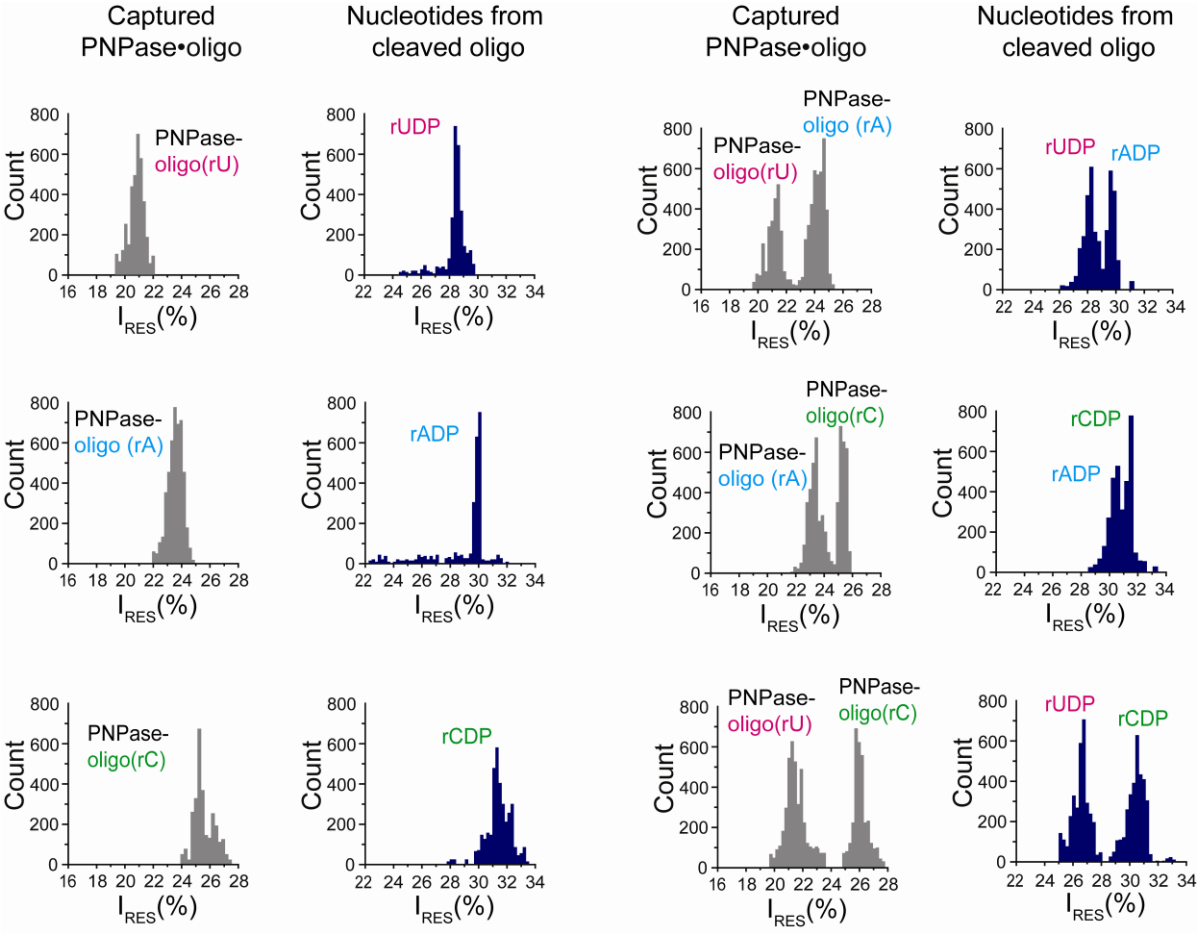


**Figure S10.** PNPase•RNA capture and cleavage within the αHL M113R-RL2 pore at +140 mV. (*Left*) $I_{RES\%}$ event histograms for PNPase•RNA captured within the αHL M113R-RL2 pore at +140 mV. oligo(rA)$_{30}$, oligo(rC)$_{30}$ and oligo(rU)$_{30}$ were examined. The rNDPs liberated by PNPase (upon the addition of $P_i$ and $Mg^{2+}$) detected with the am$_7$βCD adapter (trans) at +140 mV. *(Right)* $I_{RES\%}$ event histograms for PNPase•RNA captured within the αHL M113R-RL2 pore. Mixtures of two oligonucleotides were used: (*top*) oligo(rA)$_{30}$ and oligo(rU)$_{30}$; (*center*) oligo(rA)$_{30}$ and oligo(rC)$_{30}$; (*bottom*) oligo(rU)$_{30}$ and oligo(rC)$_{30}$. The rNDPs liberated by PNPase (upon the addition of $P_i$ and $Mg^{2+}$) detected with the am$_7$βCD adapter (trans) at +140 mV. $I_{RES\%}$ values are mean values (±S.D.) taken from Gaussian fits to event histograms. $I_{RES\%} = (I_{RES}/I_O) \times 100$.

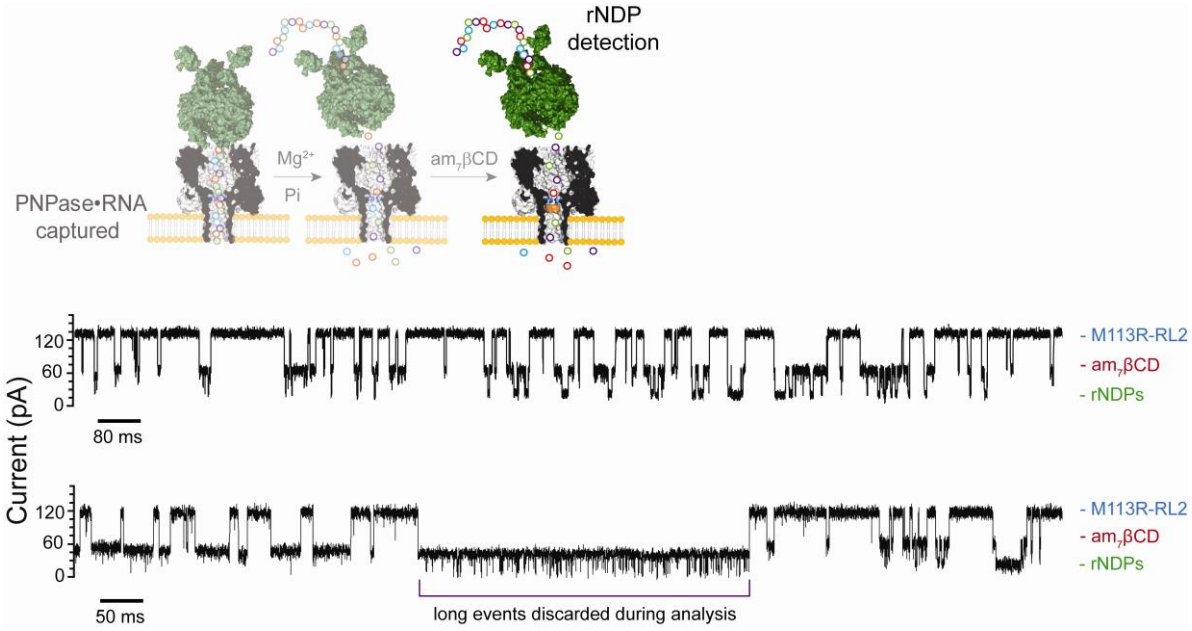


**Figure S11.** Detection of rNDPs with the $am_7\beta CD$ adapter in the αHL M113R-RL2 pore. The rNDPs liberated by PNPase (upon the addition of $P_i$ and $Mg^{2+}$) are detected with the $am_7\beta CD$ adapter (80 μM, trans) at +120 mV. The traces were recorded in 1.2 M KCl, 25 mM Tris-HCl, at pH 6.0, in the presence of PNPase and hetero-oligomeric ssRNA ($oligo(het)_{30}$: 3'-[r]AAAUGGACUGGCUUCGGAAGCCAAAUGGAU-5') (cis). Current blockades >100 ms (as shown in the lower current trace) were discarded from analysis. A histogram of the data from this experiment is shown in Figure 4f.

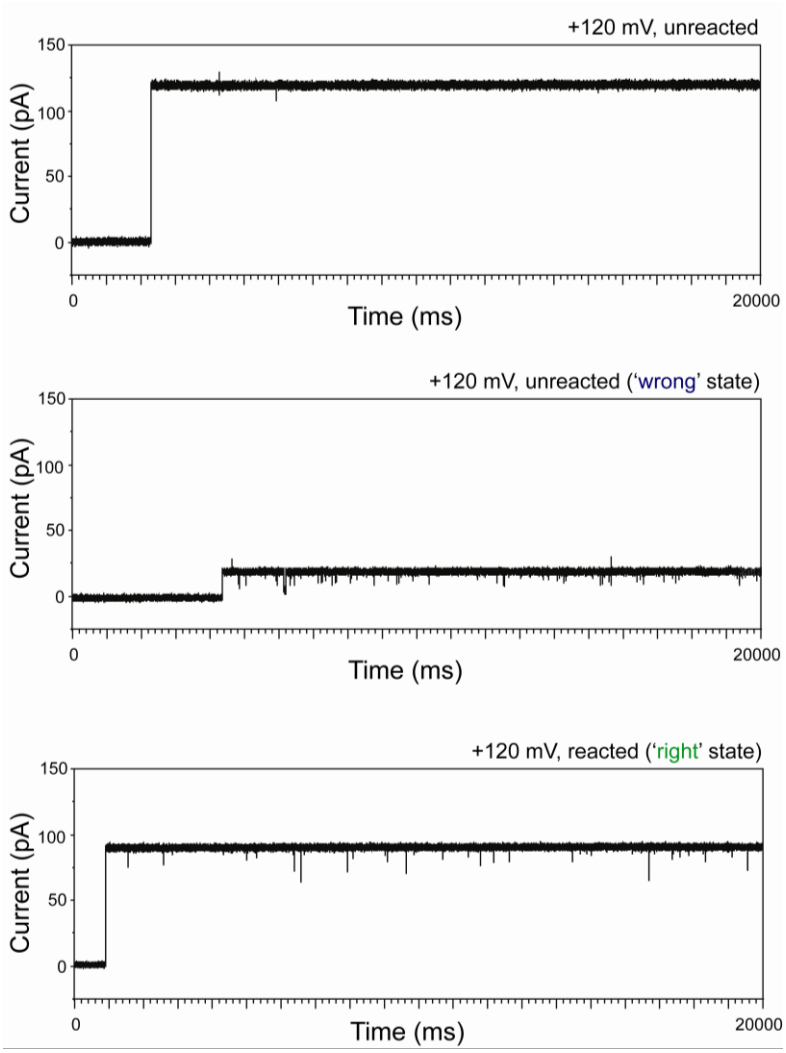


**Figure S12.** Representative single-channel recordings showing the insertion of αHL-$(N139Q)_6(N139Q/L135C)_1$.$am_6$-amPDP$_1$-βCD pores into the lipid bilayer at +120 mV in 1 M KCl, 25 mM Tris-HCl, at pH 7.5. Three predominant classes of events were observed. 30% of the pores contained no CD (top panel); 10% of the pores gave noisy baselines with current approaching 0 pA (middle panel); 60% were judged to be correctly constructed pores (bottom panel). The latter were characterized by a lower current value (~50% less) than what is seen for the (i) case, due to the presence of the CD. Here, the current remained constant, and the pore was not closed or removed by changing the polarity or magnitude of the applied potential. Only these pores were used for the identification of rNDPs.

## Supporting References


1. Cheley, S.; Braha, O.; Lu, X.; Conlan, S.; Bayley, H. *Protein Sci* **1999,** 8, (6), 1257-67.

2. Maglia, G.; Restrepo, M. R.; Mikhailova, E.; Bayley, H. *Proc Natl Acad Sci U S A* **2008,** 105, (50), 19720-5.

3. Clarke, J.; Wu, H.-C.; Jayasinghe, L.; Patel, A.; Reid, S.; Bayley, H. *Nat Nano* **2009,** 4, (4), 265-270.

4. Hardwick, S. W.; Gubbey, T.; Hug, I.; Jenal, U.; Luisi, B. F. *Open Biology* **2012,** 2, (4).

5. Yuan, D.-Q.; Izuka, A.; Fukudome, M.; Rekharsky, M. V.; Inoue, Y.; Fujita, K. *Tetrahedron Letters* **2007,** 48, (19), 3479-3483.

6. Montal, M.; Mueller, P. *P Natl Acad Sci USA* **1972,** 69, (12), 3561-3566.

7. Stoddart, D.; Heron, A. J.; Mikhailova, E.; Maglia, G.; Bayley, H. *Proc Natl Acad Sci U S A* **2009,** 106, (19), 7702-7.

8. Ayub, M.; Bayley, H. *Nano Lett* **2012,** 12, (11), 5637-5643.